International Game Theory Review, Vol. 8, No. 1 (2006) 1–20

World Scientific
www.worldscientific.com

GLOBAL BIFURCATIONS IN DUOPOLY WHEN THE COURNOT POINT IS DESTABILIZED VIA A SUBCRITICAL NEIMARK BIFURCATION

ANNA AGLIARI*

Dip. Scienze Economiche e Sociali, Catholic University
Via Emilia Parmense, 84. Piacenza I-29100 Italy
anna.agliari@unicatt.it

LAURA GARDINI

Dip. Scienze Economiche, University of Urbino "Carlo Bo"
Urbino I-61029 Italy
gardini@econ.uniurb.it

TONU PUU

Dep. Economics University of Umea
Umea SE-90187 Sweden
Tonu.Puu@econ.umu.se

An adaptive oligopoly model, where the demand function is isoelastic and the competitors operate under constant marginal costs, is considered. The Cournot equilibrium point then loses stability through a subcritical Neimark bifurcation. The present paper focuses some global bifurcations, which precede the Neimark bifurcation, and produce other attractors which coexist with the still attractive Cournot fixed point.

Keywords: Duopoly model; Subcritical Neimark bifurcation; Border collision bifurcation.

Subject Classification: 37N40, 70K, 37G99

1. Introduction

Oligopoly theory, founded in 1838 by Cournot, Cournot (1938), is one of the oldest, if not *the* oldest branch of mathematical economics. It is also one of the oldest dynamic theories in economics that were suspected to lead to complex dynamic phenomena. Rand (1978) suggested that if the reaction functions of the competitors were of the shape known from the logistic iteration, i.e., first increasing and then decreasing, then duopoly theory would be capable of producing all known phenomena of complex dynamics: orbits of any periodicity, as well as quasiperiodic and chaotic ones, along with multistability of attractors.

*Corresponding author.

In traditional industrial organization textbooks the reaction functions are always drawn as simple straight lines, so no interesting dynamic phenomena at all appear at the average economics student's horizon. However, there exist many circumstances under which the shapes suggested by Rand can arise. One of the simplest is maybe the case suggested in Puu (1991): an isoelastic demand curve, combined with constant marginal costs for the duopolists.

The isoelastic demand curve (of unit elasticity) itself arises whenever the consumers maximize utility functions of the popular Cobb-Douglas variety. As is well known, the consumers then spend fixed budget shares on each commodity, so the demand for any commodity becomes reciprocal to the price of this particular commodity (independently of the prices of all the other commodities).

This reciprocity, for once, also makes aggregation over individual consumers an easy matter, and so aggregate demand as well retains this property of reciprocity to price. Constant marginal costs, likewise, belong to the simplest first approximations in microeconomic models.

In Puu (1991) it was shown that under these assumptions a period doubling cascade to chaos occurs when the competitors react in the Cournot mode. It was also shown that, making the adjustment process adaptive, i.e., assuming that the competitors move to a weighted average of their previous moves and their calculated new best responses according to Cournot, results in the loss of stability occurring through a Neimark bifurcation. So, once the fixed point loses stability, it is replaced by a periodic solution, or by a closed orbit in phase space.

There is a special characteristic to this Neimark bifurcation: it is not supercritical, but subcritical. So, it is not the loss of stability for the fixed Cournot point that gives rise to another attractor. Rather, this other attractor (or several of them) exist even before the Neimark bifurcation, so at the bifurcation moment, the fixed point just loses stability through the collapse of its basin of attraction around it, thus eliminating the fixed point itself from the list of attractors. Before this, there is coexistence, or multistability.

This also shows up in the bifurcation diagrams, where the periodic Arnol'd tongues protrude right through the Neimark bifurcation curve. For illustrations see Puu (2003).

All this means that the global bifurcations, through which multistability arises, producing other attractors along with the Cournot point, is more interesting than the Neimark bifurcation itself, which just signifies the final destabilization of the fixed point.

The objective of the present paper is a more close study of this emergence of multistability preceding the subcritical Neimark bifurcation in oligopoly models of the type described.

One of the peculiarity of these models is the piecewise smooth character of the map, and it is well known that for this kind of maps particular bifurcation are involved, due to the change of definition of the map. Such bifurcations are related with closed invariant sets (as attractors, frontiers, manifolds) having a contact with

the border of a region of definition of the map. Since the papers by Nusse and Yorke, Nusse and Yorke (1992), Nusse *et al.* (1994), Nusse and Yorke (1995), a common term to refer to this type of bifurcation is "*border collision*". Indeed, we shall see also in this model that appearance/disappearance of closed invariant sets are associated with border collision bifurcations.

It is worth stressing that subcriticality which occurs in our model is not just a mathematical property, it also has considerable significance in terms of economic substance. This is because, with subcriticality, the bifurcations become "hard", so that the trajectory makes a jump to approach some distant attractor, and cannot be stabilized towards the Cournot point again through any fine tuning.

The structure of the paper is as follows. In Sec. 2 we introduce the Cournot duopoly model and we analyze the properties of the map that governs the adjustment process. In particular we prove that a subcritical Neimark bifurcation of the fixed point occurs. In Sec. 3 we show a border collision bifurcation which leads to the emergence of a closed repelling invariant curve Γ, whose shrinking process causes the loss of stability of the Cournot equilibrium point. Such a border collision gives rise also to an attracting invariant closed curve which coexists with the attracting equilibrium point. In Sec. 4 we show that more complex multistability situations, always due to border collision bifurcations, are possible.

2. The Model

Consider a market in which the demand function is isoelastic, i.e.,

$$Q = \frac{1}{p}, \tag{1}$$

Q denotes total demand and p the price of the commodity.

Moreover, assume there are two competitors in the market, producing under a technology of constant marginal costs, denoted a and b. Following the Cournot hypothesis, the competitors act simultaneously, choosing their outputs q_i. We assume they have no capacity constraints, so $q_i \in [0, +\infty)$, $i = 1, 2$.

The inverse demand function is $p = 1/Q$, where $Q = q_1 + q_2$. Hence, $p = 1/(q_1 + q_2)$, so the profit function of producer 1 becomes

$$U_1(q_1, q_2) = \frac{q_1}{q_1 + q_2} - aq_1 \tag{2}$$

and his optimal production, given the expected production q_2^e of the competitor, is the solution to the problem

$$\max_{q_1 \geq 0} U_1(q_1, q_2^e). \tag{3}$$

From Eq. (3), it is easy to obtain the best response of producer 1:

$$R_1(q_2^e) = \begin{cases} \sqrt{\frac{q_2^e}{a}} - q_2^e & \text{if } 0 \leq q_2^e \leq \frac{1}{a} \\ 0 & \text{if } q_2^e > \frac{1}{a} \end{cases}. \tag{4}$$

The best response of producer 2 can be obtained analogously:

$$R_2(q_1^e) = \begin{cases} \sqrt{\frac{q_1^e}{b}} - q_1^e & \text{if } 0 \le q_1^e \le \frac{1}{b} \\ 0 & \text{if } q_1^e > \frac{1}{b} \end{cases} . \tag{5}$$

$R_1(q_2^e)$ and $R_2(q_1^e)$ are normally called the reaction functions of the competitors. If we identify actual and expected outputs, then $R_1(q_2)$ and $R_2(q_1)$ represent curves in the q_1, q_2 plane, which intersect at the origin and in the Cournot equilibrium point.

If the competitors have perfect foresight, and if they do not try any smart strategy for instance of the Stackelberg type, they immediately jump to the Cournot equilibrium point, whose coordinates are easily calculated:

$$E^* = (q_1^*, q_2^*) = \left(\frac{b}{(a+b)^2}, \frac{a}{(a+b)^2} \right). \tag{6}$$

Observe that for each firm this equilibrium point is a decreasing function of its own marginal cost, and, seen as a function of the marginal cost of the competitor, attains its maximum when $b = a$.

If we adopt the "myopic rationality" of Cournot's original setup, then each of the firms assumes the output of the competitor to remain the same as it was in the previous period, i.e.

$$q_i^e(t) = q(t-1). \tag{7}$$

Using this convention, we could also set up a dynamic process in which the Cournot equilibrium point is reached, not in one step, but approached asymptotically through successive adjustments according to the reaction functions (4)–(5). This, of course, only holds provided the Cournot equilibrium point is stable. As indicated in the introduction, the Cournot point can be destabilized even in such a simple adjustment process, and be replaced by periodic processes or even by chaos.

However, we do not consider this at present, but adopt the adaptive format right from the outset, i.e., we assume that the competitors do not immediately aim for the optimum predicted by the myopic best reply function. As a conservative concession to their limited knowledge concerning the actual reactions of the competitor, they only adjust their previous decision in the direction of the new optimum. Thus:

$$\begin{cases} q_1(t) = (1-\lambda) q_1(t-1) + \lambda R_1(q_2(t-1)) \\ q_2(t) = (1-\mu) q_2(t-1) + \mu R_2(q_1(t-1)) \end{cases} \tag{8}$$

where we assume fixed weights, or adjustment speeds λ and μ, for the previous decision and the calculated myopic best response. Of course $0 \le \lambda, \mu \le 1$. Observe that if both adjustment speeds equal 1, then we are back to the original Cournot duopoly as verbally described above.

Substituting the best response functions (4) and (5) in (8), we obtain the map T, which is the object of the present study

$$T:\begin{cases} x' = \begin{cases}(1-\lambda)x+\lambda\left(\sqrt{\frac{y}{a}}-y\right) & \text{if } 0\le y\le \frac{1}{a}\\ (1-\lambda)x & \text{if } y>\frac{1}{a}\end{cases}\\ \\ y' = \begin{cases}(1-\mu)y+\mu\left(\sqrt{\frac{x}{b}}-x\right) & \text{if } 0\le x\le \frac{1}{b}\\ (1-\mu)y & \text{if } x>\frac{1}{b}\end{cases}\end{cases}. \tag{9}$$

In Eq. (9), as in the rest of the discussion, we use the variables x and y to denote the quantities q_1 an q_2, and the prime symbol ($\prime$) to denote the unit advancement operator, i.e., if x is the decision of producer 1 at time $t-1$, $q_1(t-1)$, then x' denotes $q_1(t)$.

The two-dimensional map T is continuous and piecewise smooth in the plane $\mathbb{R}^2_+$. It depends on four parameters, the marginal costs $a>0$ and $b>0$ and the adjustment speeds λ and μ, both constrained to the interval $[0,1]$.

But it is possible to show that in order to study the dynamical behaviour of T, only three parameters are essential. Without loss of generality, we can fix any of the marginal costs at the value 1, for instance the smaller of them, because the following proposition holds:

Proposition 1. *The map T with parameters (a,b,λ,μ) is topologically conjugated to the map $\widetilde{T}$ with parameters $(\tau a,\tau b,\lambda,\mu)$, $\tau>0$, via the homeomorphism $\Phi(x,y)=(\tau x,\tau y)$.*

Proof. We have

$$\begin{aligned} T(\Phi(x,y)) &= \begin{pmatrix} \begin{cases}(1-\lambda)\tau x+\lambda\left(\sqrt{\frac{\tau y}{a}}-\tau y\right) & \text{if } 0\le \tau y\le \frac{1}{a}\\ (1-\lambda)\tau x & \text{if } \tau y>\frac{1}{a}\end{cases}\\ \begin{cases}(1-\mu)\tau y+\mu\left(\sqrt{\frac{\tau x}{b}}-\tau x\right) & \text{if } 0\le \tau x\le \frac{1}{b}\\ (1-\mu)\tau y & \text{if } \tau x>\frac{1}{b}\end{cases}\end{pmatrix}\\ &= \begin{pmatrix} \begin{cases}\tau\left[(1-\lambda)x+\lambda\left(\sqrt{\frac{y}{\tau a}}-y\right)\right] & \text{if } 0\le y\le \frac{1}{\tau a}\\ \tau(1-\lambda)x & \text{if } y>\frac{1}{\tau a}\end{cases}\\ \begin{cases}\tau\left[(1-\mu)y+\mu\left(\sqrt{\frac{x}{\tau b}}-x\right)\right] & \text{if } 0\le x\le \frac{1}{\tau b}\\ \tau(1-\mu)y & \text{if } x>\frac{1}{\tau b}\end{cases}\end{pmatrix}\\ &= \Phi(\widetilde{T}(x,y))\,. \end{aligned}$$

□

In what follows we consider $b=1$ and $a>1$ so the map T in Eq. (9) becomes

$$T:\begin{cases} x' = \begin{cases}(1-\lambda)x+\lambda\left(\sqrt{\frac{y}{a}}-y\right) & \text{if } 0\le y\le \frac{1}{a}\\ (1-\lambda)x & \text{if } y>\frac{1}{a}\end{cases}\\ \\ y' = \begin{cases}(1-\mu)y+\mu\left(\sqrt{x}-x\right) & \text{if } 0\le x\le 1\\ (1-\mu)y & \text{if } x>1\end{cases}\end{cases}. \tag{10}$$

2.1. *The equilibrium point and local stability analysis*

As we observed, the map T in Eq. (10) is piecewise smooth. This means that we need to consider four maps, defined in four different regions of $\mathbb{R}^2_+$. More precisely, write

$$\mathbb{R}^2_+ = R_1 \cup R_2 \cup R_3 \cup R_4 \tag{11}$$

where

$$\begin{aligned} &R_1 = [0,1] \times \left[0, \frac{1}{a}\right]; \quad R_2 = (1,+\infty) \times \left[0, \frac{1}{a}\right]; \\ &R_3 = (1,+\infty) \times \left(\frac{1}{a}, +\infty\right); \quad R_4 = [0,1] \times \left(\frac{1}{a}, +\infty\right). \end{aligned} \tag{12}$$

In each region R_i the composite map T is given by a different map T_i.

The simplest is

$$T_3 : \begin{cases} x' = (1-\lambda)x \\ y' = (1-\mu)y \end{cases} \tag{13}$$

which is linear, with an attracting fixed point at $(0,0)$. But the origin does not belong to region R_3 where T_3 applies. After a finite number of iterations each trajectory starting in R_3 leaves that region.

In region R_2 we have the map

$$T_2 : \begin{cases} x' = (1-\lambda)x + \lambda\left(\sqrt{\frac{y}{a}} - y\right) \\ y' = (1-\mu)y \end{cases}. \tag{14}$$

This too always admits a fixed point at the origin, which again does not belong to R_2. We observe that at each iteration a contraction of the y value occurs (remember that $0 \le \mu \le 1$). So y tends towards 0, and $y = 0$ is an attracting direction for the fixed point $(0,0)$. Then a trajectory starting in R_2 leaves that region entering in R_1 after a finite number of steps. Similarly the map

$$T_4 : \begin{cases} x' = (1-\lambda)x \\ y' = (1-\mu)y + \mu\left(\sqrt{x} - x\right) \end{cases} \tag{15}$$

admits as fixed point the origin, not belonging to R_4, and it contracts the x value. Then a trajectory starting in R_4 after a finite number of iterations enters R_1.

Thus we conclude that, after a finite number of iterations, every trajectory enters R_1, and so the asymptotic behaviour of T strongly depends on the map

$$T_1 : \begin{cases} x' = (1-\lambda)x + \lambda\left(\sqrt{\frac{y}{a}} - y\right) \\ y' = (1-\mu)y + \mu\left(\sqrt{x} - x\right) \end{cases}. \tag{16}$$

As we will see, the region R_1, however, is not a trapping set for the map T. Hence a trajectory can escape from R_1, but, if so, it has to re-enter this region

(in a finite number of steps). This leads us to state that the attracting sets for the map T must belong to or intersect the region R_1. More precisely, when the attractor is a fixed point, it must be a fixed point of T_1 and when the orbit is periodic (or quasi-periodic) some periodic points must belong to R_1. Also in the case of chaotic behavior, a portion of the strange attractor must be contained in R_1. For this reason, in order to study the map T, we have to start from the properties of the map T_1.

The fixed points of T_1 are: the origin, always repelling, and the Cournot equilibrium point E^*, given in (6), which belongs to R_1 for every $a > 0$.

In order to study the local stability of E^*, as usual, we consider the Jacobian matrix of T_1 evaluated at the equilibrium point.

We have $J^* = \begin{bmatrix} 1-\lambda & \lambda\frac{1-a}{2a} \\ \mu\frac{a-1}{2} & 1-\mu \end{bmatrix}$, from which we can deduce the stability conditions

(1) $1 - trace(J^*) + det(J^*) = \frac{1}{4a}(a+1)^2\lambda\mu > 0$
(2) $1 + trace(J^*) + det(J^*) = 2(2-\lambda-\mu) + \frac{\mu\lambda(a+1)^2}{4a} > 0$
(3) $1 - det(J^*) = \lambda + \mu - \frac{\mu\lambda(a+1)^2}{4a} > 0.$

It is obvious that conditions 1 and 2 are always fulfilled, whereas condition 3 defines a surface in the parameter space on which a Neimark bifurcation takes place. Thus the only possible bifurcations which may occur are those related to closed invariant curves and may be very interesting in our context from an applied point of view. Moreover, in the particular case of equal adjustment speeds $\lambda = \mu$, we can prove analytically the type of the Neimark bifurcation, as stated in the following proposition.

Proposition 2. *If $\lambda = \mu < 1$, then at any crossing of the curve*

$$\lambda = \frac{8a}{(a+1)^2} \tag{17}$$

a Neimark bifurcation of subcritical type takes place.

Proof. In the case $\mu = \lambda$, denoting by S the eigenvalues, the characteristic polynomial of the Jacobian matrix J^* can be written

$$\mathcal{P}(S) = (S + \lambda - 1)^2 + \frac{1}{4a}(a-1)^2\lambda^2 . \tag{18}$$

We deduce that J^* has complex conjugated eigenvalues for every λ and a. The modulus of such eigenvalues is $|S| = (1-\lambda)^2 + \frac{1}{4a}(a-1)^2\lambda^2$, so they belong to the unit circle when (17) is fulfilled. Moreover if $\lambda < 1$, then $|S|^j \neq 1$, $j = 2, 3, 4$.

This proves that at any crossing of the curve (17) a Neimark bifurcation takes place. Finally, computing coefficients d and A (a in the book) of Theorem 3.5.2, p. 162, in Guckenheimer and Holmes (1997), we obtain $d = 1$ and $A < 0$ in the relevant parameter range. This proves that the Neimark bifurcation is of subcritical type. □

It is clear that the generic case is $\lambda \neq \mu$, however the above proposition leads to interesting dynamic situations, so that we leave the generic case for further researches and in what follows we shall focus our attention to the particular case of equal adjustment speeds for the competitors, $\mu = \lambda$, where, of course, $\lambda < 1$. In such a case we know from Proposition 2 that just before the bifurcation a repelling closed curve Γ exists while the fixed point is still attracting, and that, at the bifurcation values, it disappears, shrinking on E^*, which then becomes repelling.

The very fact that the bifurcation is subcritical has a certain importance in terms of the economics involved. Economists are most often concerned with fine tuning, i.e., keeping systems at equilibria with minute adjustments of parameters under the control of some authority. In the case of multistability and other phenomena appearing in complex nonlinear systems, this means restoring a destabilized equilibrium. It is therefore notewhorty that this never works in the case of subcritical bifurcations, because, unlike the case of supercritical bifurcations, the system jumps to some attractor at considerable distance from the original one that was destabilized.

The appearance of the repelling curve Γ involved in the subcritical Neimark bifurcation will be the object of our study. In fact the existence of such a repelling closed curve is very important, as it implies the existence of points in the phase plane with different asymptotic behaviour. Then we can expect that the Cournot equilibrium coexists with some other attractors, which, as we will see, are periodic and/or quasi-periodic (as two more attractors can exist besides the stable Cournot point). In any case, the closed curve Γ is the boundary of the immediate basin of attraction of E^*.

In particular we will see that Γ can appear with a cycle or an attracting closed curve, via a border collision bifurcation (typical of piecewise smooth maps), and that different multistability situations are possible. In our study we proceed by fixing the value of the parameter λ and letting a change.

3. Border Collision Bifurcations

In order to understand the global bifurcation causing the appearance of the closed curve Γ, we consider the map T_1 defined in Eq. (16), as noted in the previous section.

Given we are particularly interested in T_1 with $\lambda = \mu$, let us rewrite the map accordingly:

$$T_1 : \begin{cases} x' = (1-\lambda)x + \lambda\left(\sqrt{\frac{y}{a}} - y\right) \\ y' = (1-\lambda)y + \lambda\left(\sqrt{x} - x\right) \end{cases} \tag{19}$$

Due to the appearance of the square root, it is obvious that T_1 is defined only at points belonging to the nonnegative quadrant of the plane $\mathbb{R}^2$. Let us now define

the *feasible region* F_1. This is the set of points in the plane defined by

$$F_1 = \{(x, y) : x \geq 0, y \geq 0\} \tag{20}$$

Note that the feasible region is larger than the region in which the map T_1 is well defined. Indeed, we can only say that T_1 is "a map" in D if, given any initial condition $(x_0, y_0) \in D$, we have that $T_1^n(x_0, y_0)$ exists and is feasible for any n. In other words D is a region in which T_1 is defined forever in its forward iterations. This set D includes the basins of attraction of the attracting sets of the map.

In this section we shall describe the shape of D, and in particular of its boundary. We shall see that this boundary may be the repelling invariant closed curve Γ we are looking for.

In the case of noninvertible maps, such as the one we are interested in, the study of the basins of attraction can be performed using the *Riemann foliation* of the phase plane as defined by the map. Recall that, according to the literature on noninvertible maps (see Gumowski and Mira (1980), Mira *et al.* (1996)), a *Riemann foliation of the plane* means superposed "sheets", which cover the plane and explain the number of preimages that exist in its different parts.

Usually, this information is obtained considering the critical curve LC of the noninvertible map, which separates regions of the phase plane that have different numbers of rank-1 preimages. These regions are denoted Z_i, where the index i denotes the number of distinct rank-1 preimages of any point in that region. The critical curve LC is the locus of points having two merging preimages. In our case it can be obtained as the image by T_1 of the set of points for which the Jacobian determinant $|J|$ vanishes. (This set itself is denoted LC_{-1}, and is called critical curve of rank-1).

We have

$$\begin{aligned} |J| &= \det \begin{bmatrix} 1-\lambda & \lambda\left(\frac{1}{2\sqrt{ay}} - 1\right) \\ \lambda\left(\frac{1}{2\sqrt{x}} - 1\right) & 1-\lambda \end{bmatrix} \\ &= (1-\lambda)^2 - \lambda^2 \left(\frac{1}{2\sqrt{x}} - 1\right)\left(\frac{1}{2\sqrt{ay}} - 1\right) = 0\,. \end{aligned} \tag{21}$$

Solving for the variable y in explicit form, we obtain LC_{-1}:

$$\begin{cases} y = \frac{1}{4a}\left(\frac{\lambda^2(2\sqrt{x}-1)}{4\lambda\sqrt{x}-2\sqrt{x}-\lambda^2}\right)^2 \\ 0 \leq x \leq \frac{1}{4} \end{cases}. \tag{22}$$

An example of this curve is shown in Fig. 1, along with its image $LC = T_1(LC_{-1})$.

For the map T_1 the critical line LC is not enough to give the *Riemann foliation*, because of the square root in its definition. In fact, we have to take into consideration that some preimages may be unfeasible, i.e., they can have a negative coordinate. To define the regions Z_i properly, we must therefore also consider the images by T_1

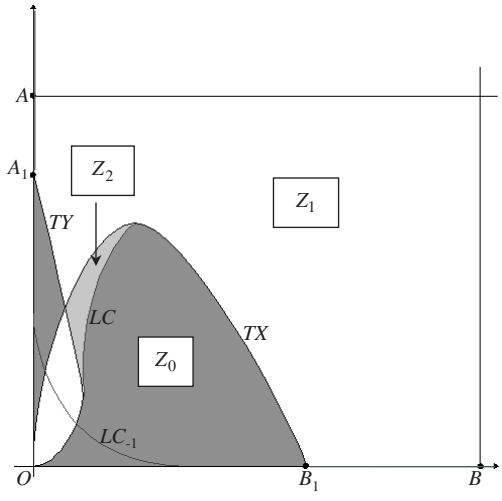

Fig. 1. Riemann foliation of the phase plane defined by the map T_1. In white the region Z_1, in grey the region Z_0 and in pale grey the small region Z_2.

of the coordinate axes, i.e., of the boundary of the set F_1. The images of these two curves $TX = T_1(\{y = 0\})$ and $TY = T_1(\{x = 0\})$ are obtained as

$$\begin{cases} TX : y = \lambda\Big(\sqrt{\frac{x}{1-\lambda}} - \dfrac{x}{1-\lambda}\Big) \\ TY : x = \lambda\Big(\sqrt{\frac{y}{a(1-\lambda)}} - \dfrac{y}{1-\lambda}\Big) \end{cases} . \tag{23}$$

The curves TX and TY are not critical lines in the sense of Gumowski and Mira (1980) and Mira *et al.* (1996), because their points do not have merging preimages. However the essential features of the critical curves theory apply also to such curves because the crossing through them still causes the appearance (or disappearance) of a rank-1 preimages. In Fig. 1 we show the regions Z_0, Z_1 and Z_2 so obtained. In particular we observe that the points of the y-axis that have admissible forward images belong to the segment OA, where O is the origin and A is the point $(0, \frac{1}{a})$. Likewise, those of the x-axis belong to the segment OB, where B is the point $(1, 0)$. This fact has a trivial explanation: 1 and $1/a$ are the supply quantities of the respective firms, for which the competitor's maximum profits turn negative.

We also observe that, consequently, the points of the y-axis having preimages belong to the half-line starting from $A_1 = T(A)$, and those of the x-axis to the half-line starting from $B_1 = T(B)$.

Let us now return to the set D. In order to obtain the boundary of D we reason as follows. Starting from F_1, i.e., the feasible region of T_1^1, we can compute F_2, the feasible region of T_1^2. This is the subregion of F_1, such that not only (x, y), but also $(x_1, y_1) = T_1(x, y)$, are feasible, so that we are able to compute T_1^2. Thus

$$F_2 = \{(x, y) \in F_1 : T_1(x, y) \in F_1\} . \tag{24}$$

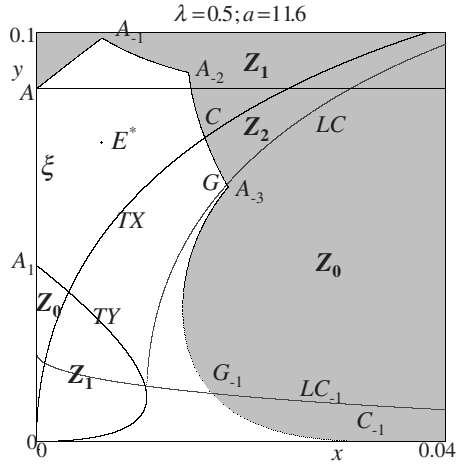

Fig. 2. The set D (white points) is the basin of attraction for the Cournot equilibrium point E^*, and it coincides with F_4. Its boundary is made up by four preimages of the segment A_1A of the y-axis, denoted by ξ.

Clearly $F_2 \subseteq F_1$, and the boundary of F_2 contains the rank-1 preimages of the boundary of F_1, as well as a portion of ∂F_1 itself. This means that a point belonging to ∂F_2 is either mapped into ∂F_1 or it belongs to F_1.

And so forth:

$$F_k = \{(x, y) \in F_{k-1} : T_1(x, y) \in F_1\}. \tag{25}$$

It may occur that a finite k exists such that $F_{k+1} = F_k = D$, as in the case displayed in Fig. 2. In this picture, obtained at $\lambda = 0.5$ and $a = 11.6$, the set D is the basin of attraction for the Cournot equilibrium point E^*, and it coincides with F_4. Its boundary is made up by four preimages of the segment A_1A of the y-axis, denoted by ξ.

Indeed, the segment ξ belongs to Z_1: its rank-1 preimage is bounded by A and A_{-1} (the rank-1 preimage of A), and it is always located in Z_1, up to the line $y = 1/a$ (and then we deduce that R_1 is not a trapping set for T_1). There exists a rank-2 preimage of ξ, bounded by A_{-1} and A_{-2}, which always belongs to Z_1. Only a portion of the preimages of rank-3 of ξ belong to Z_1. Its upper part is bounded by A_{-2} and C (a point on the curve TX), whereas the portion bounded by C and G (located on LC) belongs to Z_2 and a small portion (bounded by G and A_{-3}) to Z_0. This means that there exist rank-1 preimages of the portion $A_{-2}G$, which are rank-4 preimages of ξ. The portion CG has an extra preimage, located below the LC_{-1} curve, and it has an extremum on the x-axis. Such preimages belong to Z_0, and this completes the construction of $\partial D = \partial F_4$.

Observe that, due to the high marginal cost a, only the preimages of the y-axis are involved in the construction of the set ∂D. For a smaller value of a, the boundary of D would also be made up by the preimages of the segment B_1B, and

this occurs when the point C does not exist and the preimages of ξ have no longer a contact with the curve TX.

Obviously the structure of the set D can also be more complex, for instance, it can become disconnected, due to further contacts of its frontier with LC, but this is beyond the scope of the present paper.

It is interesting that, as the parameter a is increased, a greater number of preimages are involved in the construction of ∂D, i.e., $F_{k+1} = F_k$ for $k > 4$, and a "cyclical appearance" of new preimages shows up due to contact bifurcations of the frontier with the curve TY.

Let us clarify using some examples, always obtained for $\lambda = 0.5$. In the first case, displayed in Fig. 3(a), the mechanism we consider is not yet working, but its "germ" just comes into existence: We can see that a portion of the rank-4 preimage of ξ belongs to Z_2, and that some of its preimages belong to Z_1 and Z_2, so the preimage of rank-6 of ξ, ξ_{-6}, exists.

Well, it is just ξ_{-6} (now located close to the y-axis in the Z_0 region), and its contacts with TY, that are responsible of the quick appearance for six new preimages, which rotate around and inside the set F_6. Moreover, at each contact of a new preimage of rank-6n ($n = 1, 2, \ldots$) with TY, the same mechanism applies. For instance, in Fig. 3(b) (where D is a disconnected set), we can observe that a great number (but always a multiple of six) of preimages of ξ are needed to obtain the boundary of D. A consequence of the increasing number of preimages is that the set ∂D becomes more smooth.

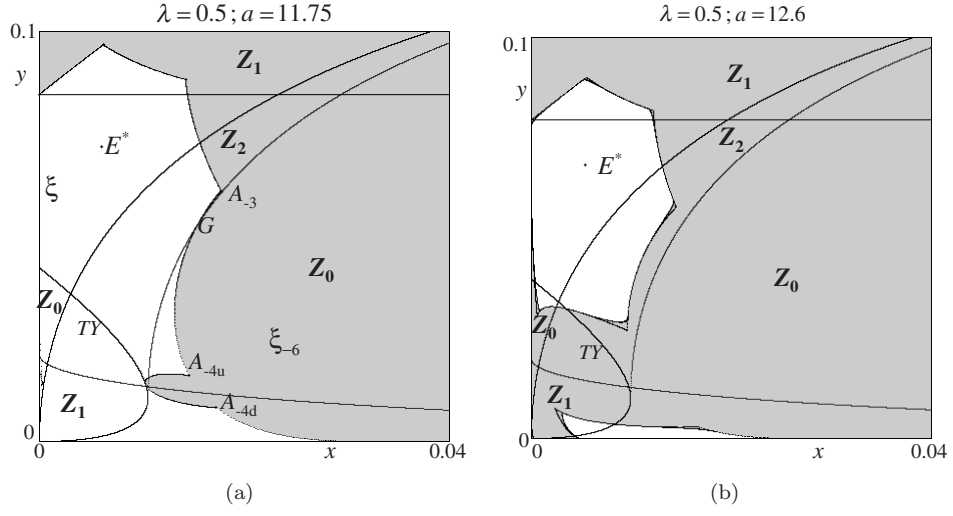

Fig. 3. (a) The bifurcation "germ" just comes into existence: A portion of the rank-4 preimage of ξ belongs to Z_2, and some of its preimages belong to Z_1 and Z_2, so the preimage of rank-6 of ξ, ξ_{-6}, exists. (b) After the contact of ξ_{-6} with TY, a greater number (but always a multiple of six) of preimages of ξ are needed to obtain the boundary of D. As a consequence the set ∂D becomes more smooth.

As the parameter a is increased further, a global bifurcation occurs, after which the boundary of D is made up by infinitely many preimages of the segment A_1A. This must be due to the appearance of two cycles (evidently of high order and therefore difficult to be identified), a saddle and a repelling node, whose saddle connection (the stable set of the saddle connecting to the repelling node) defines a closed repelling invariant curve Γ. This curve is unstable, and bounds the set D, the basin of attraction of the fixed point.

We can observe such a global bifurcation in Fig. 4(a), where there exists a preimage of the segment A_1A of a rank greater than 17, tangent to the curve TY. This means that no point of such a preimage falls into Z_0, so the process of backward iteration of A_1A never ends, i.e., there exist infinitely many preimages. We conclude that in such a case $F_{k+1} \subset F_k$ for every k, and that the set ∂D, i.e., the repelling curve Γ, is the limit set of ∂F_k as $k \to \infty$, which may also be defined as the limit set of $T_1^{-k}(\partial F_1) = T_1^{-k}(A_1A)$. An alternative way to check such a global bifurcation is to consider the forward iteration of the upper part of TY, denoted η in Fig. 4(b): We know that ∂D is tangent to η at the point P, hence its first forward iterate $T_1(\eta)$ must be tangent to ∂D in $P_1 = T_1(P)$, and so forth ... At the bifurcation value, all the forward iterates of η are tangent to ∂D, as in Fig. 4(b), obtained immediately after the bifurcation (where only a finite number of forward iterates are shown).

After the bifurcation, at a higher value of a, the repelling closed curve always exists, it becomes smaller with no contact with the curve η and, consequently, with the y-axis, that is, it is internal to the quadrant F_1 (see Fig. 5).

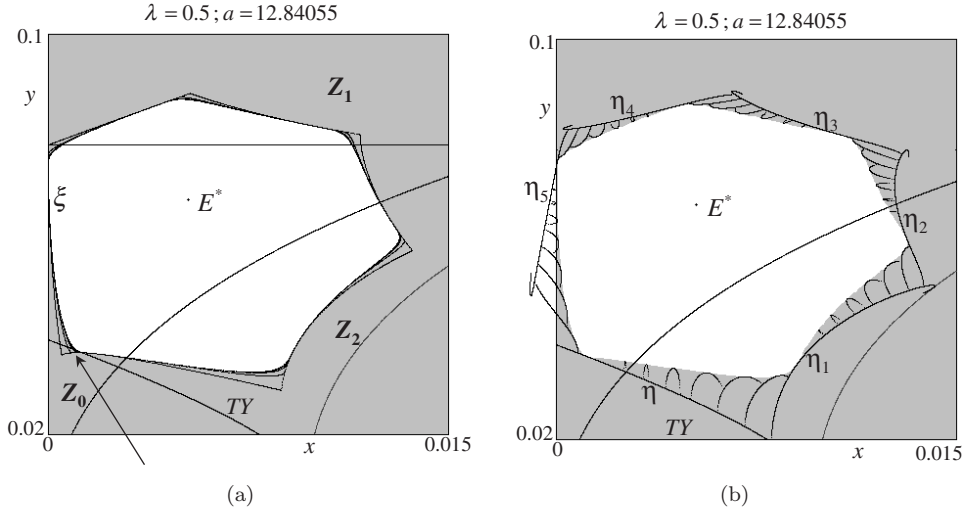

Fig. 4. (a) A preimage of the segment A_1A is tangent to the curve TY, then there exist infinitely many preimages of A_1A; now $F_{k+1} \subset F_k$ for every k, and the set ∂D, i.e., the repelling curve Γ, is the limit set of ∂F_k as $k \to \infty$. (b) An alternative way to check such a global bifurcation: all the forward iterates of η (the upper part of TY) are tangent to ∂D.

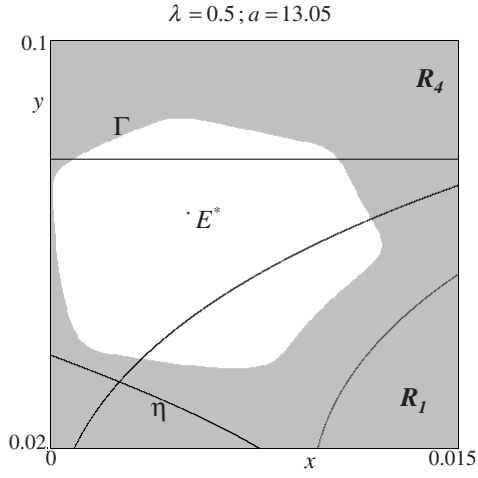

Fig. 5. The repelling closed curve Γ is internal to the quadrant F_1 and belongs to the region $R_1 \cup R_4$.

We have thus seen that either ∂D is made up by a finite number of pieces of curves belonging to $T_1^{-k}(\partial F_1)$, or (when a pair of cycles exist, giving rise to the unstable closed curve Γ) ∂D is made up by Γ itself, which is the limit set of $T_1^{-k}(\partial F_1)$ as $k \to \infty$.

As a increases, the region D shrinks more and more, merging with the fixed point at the Neimark-Hopf bifurcation value.

Let us now return to the map T, in order to show how the sequence of bifurcations just described also implies a global bifurcation for that map.

When it appears, the closed repelling curve Γ (for T_1) belongs to the region $R_1 \cup R_4$ (see Fig. 5). Then it does not influence the dynamical behaviour of T. Indeed, for the parameter constellation we considered up to now, the Cournot equilibrium point E^* is the global attractor of the trajectories for T. But, during its shrinkage process, the curve Γ has a contact with the line $y = \frac{1}{a}$, which separates the regions R_1 and R_4, as shown in Fig. 6(a). Let us denote the bifurcation value at which this happen by a_b. At $a = a_b$ a bifurcation for T, called *border collision*, takes place, which results in the appearance of an attracting closed invariant curve Γ_s, very close to the curve Γ, which now bounds the basin of attraction of the Cournot equilibrium point (see Fig. 6(b)). The effects of such a bifurcation are noticeable: The basin of attraction of the Cournot equilibrium point suddenly becomes smaller, coinciding with the set D of the map T_1, and the major part of the trajectories converge to the curve Γ_s, that is the major part of the trajectories are quasi-periodic, or periodic of high period.

We can explain this bifurcation only conjecturing that at $a = a_b$ another couple of cycles are created: a saddle and a stable node, so that now the unstable set of the saddle cycle gives rise to a closed invariant (attracting) curve on which we also have the stable cycle.

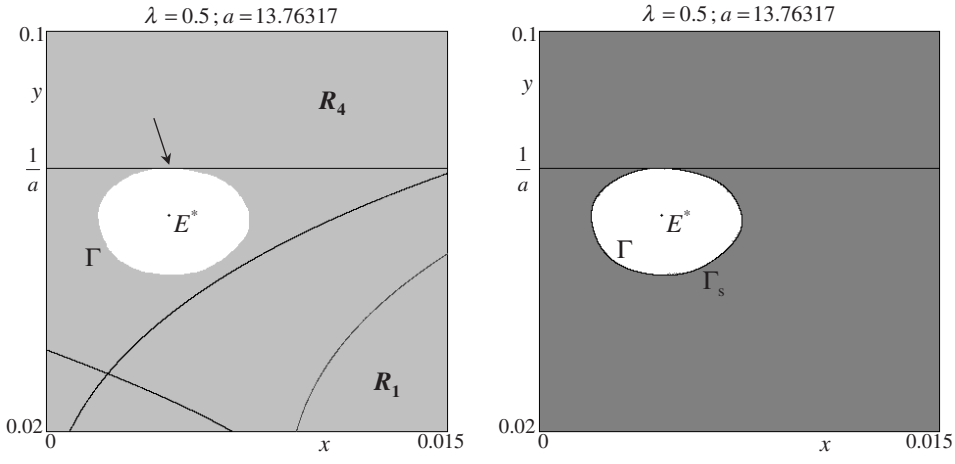

Fig. 6. (a) The curve Γ has a contact with the line which separates the regions R_1 and R_4. (b) Border collision bifurcation for the map T: An attracting closed invariant curve Γ_s appears, very close to the curve Γ, which now bounds the basin of attraction for the Cournot equilibrium point (in white). The grey points converge to Γ_s.

Once more the high periodicity of the cycles involved makes a numerical verification difficult.

The closed invariant curve Γ which bounds the basin of attraction of the fixed point E^*, as the parameter a increases, shrinks and merges with E^* at the subcritical Neimark bifurcation value a_N, leaving an unstable fixed point and an attracting set Γ_s quite far from it. It is worth to stress that this leads to an hysteresis effect: once large-amplitude oscillations have begun, they cannot be turned off by bringing a back to a_N and the system returns to the Cournot equilibrium point only if the parameter is decreased to a_b.

4. Multistability

In the previous section we have seen that the border collision bifurcation gives rise to a new attractor, and causes a drastic reduction of the basin of attraction for the fixed point. Now, analyzing a sequence of bifurcations that arise inside a periodic window, we shall see how the situations of multistability, always due to border collision bifurcations, can be even more complex.

From the bifurcation diagram for the map T, not shown here (see for instance Puu (2003), p. 278), we obtain that at $\lambda = 0.5039$ a window of period 6 exists. Then we fix this value for λ and let a vary, in order to analyze the bifurcation sequence leading to the appearance of the cycles (stable and unstable), and of the repelling closed curve Γ.

As usual we start from the map T_1. Also in this case, the sequence of bifurcations leads to a set D internal to F_1, with its boundary given by the limit set of the

preimages of the frontier of the feasible region (in a way similar to the one described in the previous section).

But now a periodic orbit, of period 6, on the repelling curve is obtained. In Fig. 7(a) we observe two cycles of period 6 on Γ: a saddle (a periodic point of which is $(0.00149, 0.0660)$ with eigenvalues $S_1 = 1.1236$, $S_2 = 0.9977$), and a repelling node (a periodic point of which is $(0.001508, 0.0666)$ with eigenvalues $S_1 = 1.1218$,

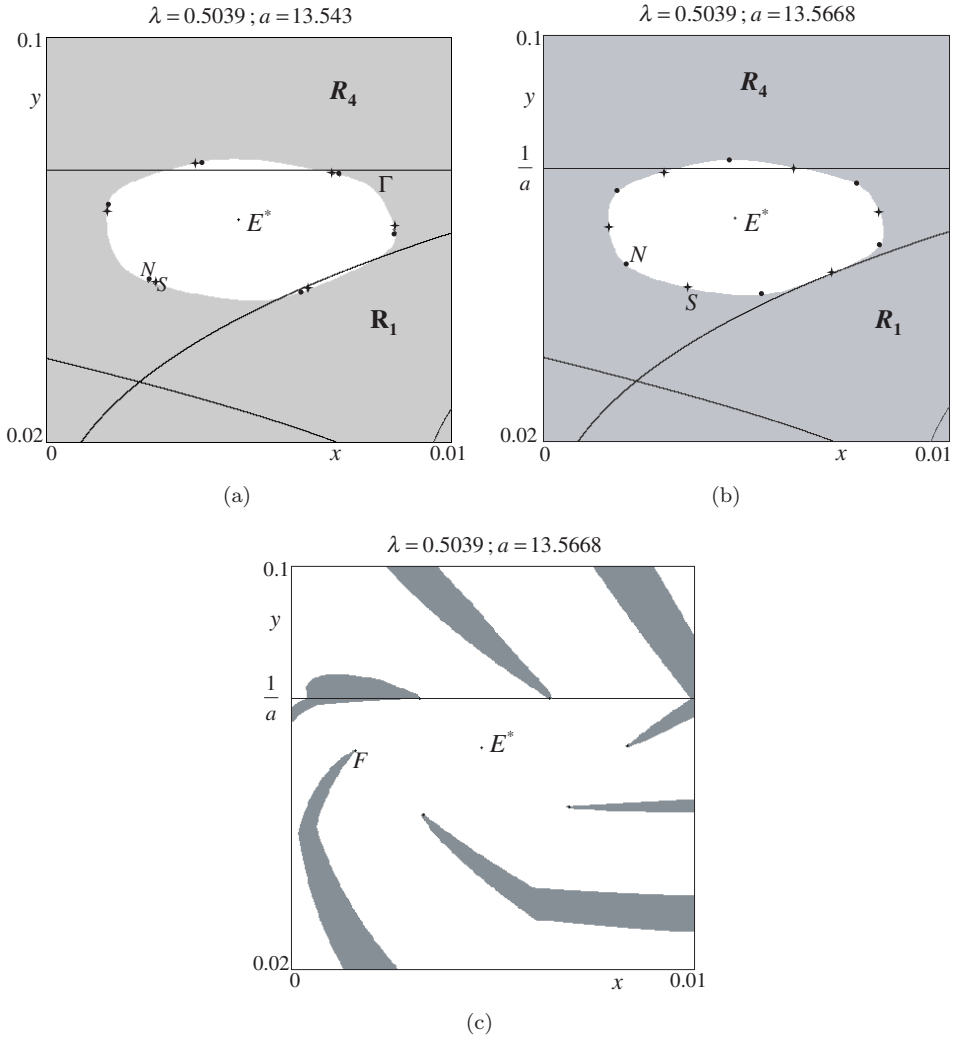

Fig. 7. (a) Two cycles of period 6 on Γ, a saddle and a repelling node node, born by a saddle-node bifurcation. The curve Γ results from a saddle connection, i.e., the stable manifold of the saddle connects the periodic points. (b) The contact between the saddle cycle and the upper bound of R_1. (c) Border collision for the map T: An attracting focus cycle of period 6 appears, as well as a saddle cycle of period 6 quite indistinguishable from the attracting one.

$S_2 = 1.0024$). Such cycles are very close to each other, because they are just born by a saddle-node bifurcation (the numerical values of the two eigenvalues S_2 close to unity confirm this). In the present situation the curve Γ results from a saddle connection, i.e., the stable manifold of the saddle connects the periodic points, forming a repelling invariant set. Observe that both the saddle and the unstable cycle have a periodic point belonging to R_4, though very close to the line $y = \frac{1}{a}$, so they do not affect the dynamic behaviour of T (for which only an attracting fixed point exists). But as the value of the parameter a is slightly increased, we can observe the contact between the saddle cycle and the upper bound of R_1 (Fig. 7(b)); as before this contact corresponds to a bifurcation for the map T. We can observe it in Fig. 7(c), where an attracting cycle of period 6 appears, reducing, though not so drastically, the basin of attraction of the Cournot equilibrium point. At $a = 13.5668$, shown in Fig. 7(c), this cycle is a focus with modulus $|\lambda| = 0.24267$ and at this parameter configuration there also exists a saddle cycle of period 6, with eigenvalues $S_1 = 1.05$ and $S_2 = 0.2835$. It is not visible in Fig. 7(c) because it is quite indistinguishable from the attracting one (and different from the saddle cycle existing for T_1). Its stable set bounds the basin of attraction of the stable cycle.

The closeness of the two cycles suggests that they are born together, but the presence of the focus and the eigenvalues do not suggest a fold bifurcation. Two possibilities are open: either an attracting node appears with the saddle at the bifurcation value (via the usual saddle-node bifurcation) and turns into a focus immediately after, or the two cycles appear via a border collision bifurcation not necessarily with an eigenvalue of unit modulus.

In any case, in the situation shown in Fig. 7(c) the attracting focus is very close to the frontier of its basin of attraction, given by the stable manifold of the saddle cycle. As a increases the basin of the fixed point becomes smaller, as we can see in Fig. 8(a), in which we also show (in pale grey) its unstable manifold. This converges to the fixed point from one side and to the attracting 6-cycle from the other.

From Fig. 8(a) we can also observe that another border collision bifurcation is emerging. We note that the unstable manifold of the saddle is very close to the frontier of the basin of attraction of E^*, and it seems to "describe" a closed curve in phase space. Indeed, looking at the map T_1, we can observe that, slightly increasing the marginal cost a, the repelling curve Γ becomes tangent to the upper bound of the region R_1 (see Fig. 8(b)). As in the previous section, the border collision leads to the appearance of an attracting curve Γ_s, close to the repelling curve Γ. Then, after the bifurcation, we have three coexisting attractors, the Cournot equilibrium point, the attracting curve and the focus cycles of period 6. Their basins of attraction are separated by the invariant repelling closed curve Γ, which separates the trajectories converging to the fixed point from the quasi periodic ones, and by the stable set of the saddle cycle, separating the periodic and the quasi-periodic trajectories (see Fig. 8(c)).

The interval of existence of the curve Γ_s is very short. A further slight increase of the parameter a leads to a contact of Γ_s with the saddle, which causes the

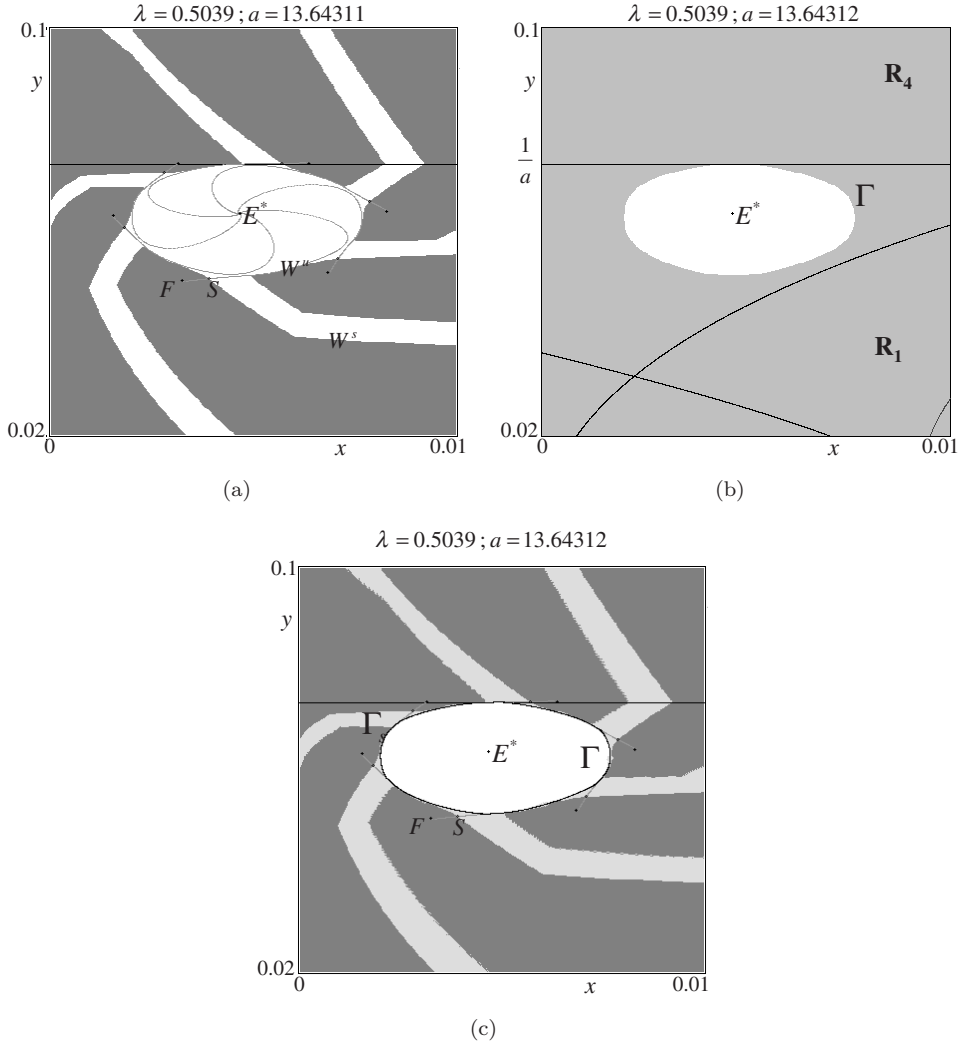

Fig. 8. (a) The basin of the fixed point is smaller. The unstable manifold of the saddle cycle (in pale grey) is very close to the frontier of the basin of attraction of E^*, and it seems to "describe" a closed curve in phase space. (b) For the map T_1, the repelling curve Γ becomes tangent to the upper bound of the region R_1: the border collision for the map T will lead to the appearance of an attracting curve Γ_s, close to the repelling curve Γ. (c) After a new border collision bifurcation, three coexisting attractors exist: the Cournot equilibrium point, an attracting curve Γ_s and the focus cycles of period 6. Their basins of attraction are separated by the invariant repelling closed curve Γ, which separates the trajectories converging to the fixed point (in white) from the quasi periodic ones (in light gray), and by the stable set of the saddle cycle, separating the periodic (in dark gray) and the quasi-periodic trajectories.

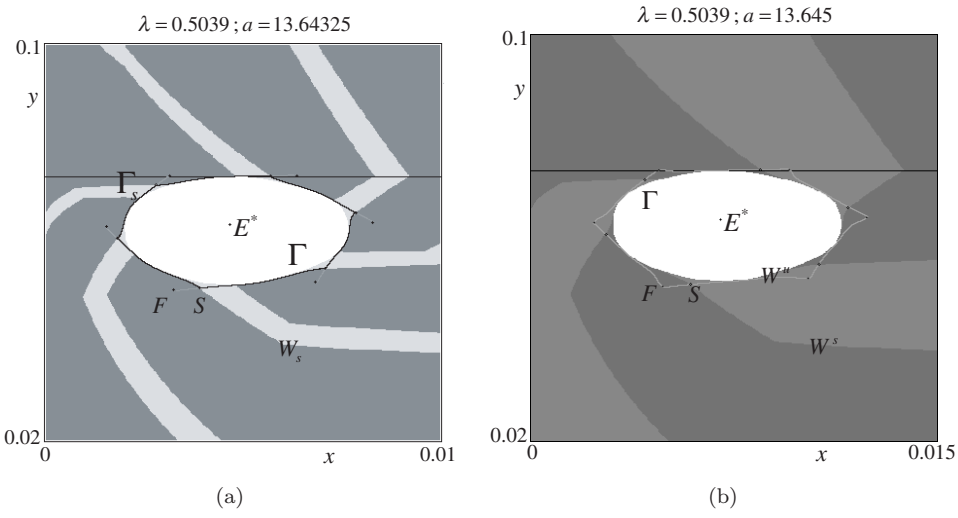

Fig. 9. (a) The contact of Γ_s with the saddle, which causes the disappearance of one attracting set. At the contact bifurcation the curve Γ_s connects all the periodic points of the saddle cycle. (b) After the contact only two invariant curves survive: a repelling one, Γ, which is the boundary of the basin of attraction of E^* and the saddle connection between the two cycles of period 6. The two colors (different gray tonalities) in the basin of attraction of the attracting 6-cycle make in evidence the stable manifold of the saddle 6-cycle.

disappearance of one attracting set. At the contact bifurcation the curve Γ_s connects all the periodic points of the saddle cycle (Fig. 9(a)), and after the contact only two invariant curves survive: a repelling one, Γ, which is the boundary of the basin of attraction of E^* and the saddle connection between the two cycles of period 6 (Fig. 9(b)). Now the unstable manifold of the saddle goes to the attracting 6-cycle, and the stable one separates the basins of the single periodic points of T^6, forming a spiral around Γ. This is shown in Fig. 9(b), obtained just after the bifurcation.

Acknowledgments

This work has been performed as one of the activities of the national research project "Nonlinear Models in Economics and Finance: Complex Dynamics, Disequilibrium, Strategic Interaction", MIUR, Italy and in the framework of the Joint Research Grant (0382) "Reconsideration of economic dynamics from a new perspective of nonlinear theory", Chuo University, Tokyo, Japan.

References

Cournot, A. [1838] *Récherches sur les Principes Mathématiques de la Théorie des Richesses* (Hachette, Paris).

Guckenheimer, J. and Holmes, P. [1997] *Nonlinear Oscillations, Dynamical Systems, and Bifurcations of Vector Fields* (Springer-Verlag, New York).

Gumowski, I. and Mira, C. [1980] *Dynamique Chaotique. Transition Ordre-Desordre* (Cepadues, Toulouse).

Mira, C., Gardini, L., Barugola, A. and Cathala, J. C. [1996] *Chaotic Dynamics in Two-dimensional Noninvertible Maps* (World Scientific, Singapore).

Nusse, H. and Yorke, J. [1992] Border-collision bifurcation including "period two to period three" for piecewise smooth systems, *Physica D* **57**, 39–57.

Nusse, H. and Yorke, J. [1995] Border-collision bifurcation for piecewise smooth one-dimensional maps, *Int. J. Bifurcations and Chaos* **5**(1), 189–207.

Nusse, H., Ott, E. and Yorke, J. [1994] Border-collision bifurcations: An explanation for observed bifurcation phenomena, *Physic Review E* **49**, 1073–1076.

Puu, T. [1991] Chaos in duopoly pricing, *Chaos, Solitons & Fractals* **1**, 573–581.

Puu, T. [2003] *Attractors, Bifurcations, & Chaos-Nonlinear Phenomena in Economics* (Springer-Verlag, New York).

Rand, D. [1978] Exotic phenomena in games and duopoly models, *J. Mathematical Economics* **5**, 173–184.